

ACCDOA: ACTIVITY-COUPLED CARTESIAN DIRECTION OF ARRIVAL REPRESENTATION FOR SOUND EVENT LOCALIZATION AND DETECTION

Kazuki Shimada, Yuichiro Koyama, Naoya Takahashi, Shusuke Takahashi, Yuki Mitsufuji
Sony Corporation, Tokyo, Japan

ABSTRACT

Neural-network (NN)-based methods show high performance in sound event localization and detection (SELD). Conventional NN-based methods use two branches for a sound event detection (SED) target and a direction-of-arrival (DOA) target. The two-branch representation with a single network has to decide how to balance the two objectives during optimization. Using two networks dedicated to each task increases system complexity and network size. To address these problems, we propose an activity-coupled Cartesian DOA (ACCDOA) representation, which assigns a sound event activity to the length of a corresponding Cartesian DOA vector. The ACCDOA representation enables us to solve a SELD task with a single target and has two advantages: avoiding the necessity of balancing the objectives and model size increase. In experimental evaluations with the DCASE 2020 Task 3 dataset, the ACCDOA representation outperformed the two-branch representation in SELD metrics with a smaller network size. The ACCDOA-based SELD system also performed better than state-of-the-art SELD systems in terms of localization and location-dependent detection.

Index Terms— Sound event localization and detection, neural-network

1. INTRODUCTION

Sound event localization and detection (SELD) involves identifying both the direction-of-arrival (DOA) and the type of sound events. SELD has played an essential role in many applications, such as surveillance [1–3], bio-diversity monitoring [4], and context-aware devices [5, 6]. Similar to sound event detection (SED) and DOA estimation, recent competitions such as DCASE challenge show significant progress in the SELD research area using neural-network (NN)-based methods [7, 8].

NN-based SELD methods can be categorized into two approaches. The first aims to integrate an NN-based SED method and a physics-based DOA estimation method [9–12]. The second, which uses only NN-based methods [13–21], performs excellently when labeled data are available [7, 8]. Adavanne *et al.* proposed SELDnet, which uses two branches for two targets: an SED target and a DOA target [13, 14]. Using the two-branch representation, SELDnet aims to solve the multi objectives with a single network. Cao *et al.* proposed a two-stage method that uses two networks: an SED network and a DOA estimation network [18]. The two-stage method uses the two single networks to concentrate on each task.

The two-branch representation with a single network has to decide the balance of the objectives. Such a multi-objective problem is commonly solved by linearly combining the losses with weights defining the trade-off between the loss terms. However, the weights' values can strongly affect the performance of the model, and their tuning can be cumbersome [22]. Although decomposing a network into two task-specific networks avoids the multi-objective problem,

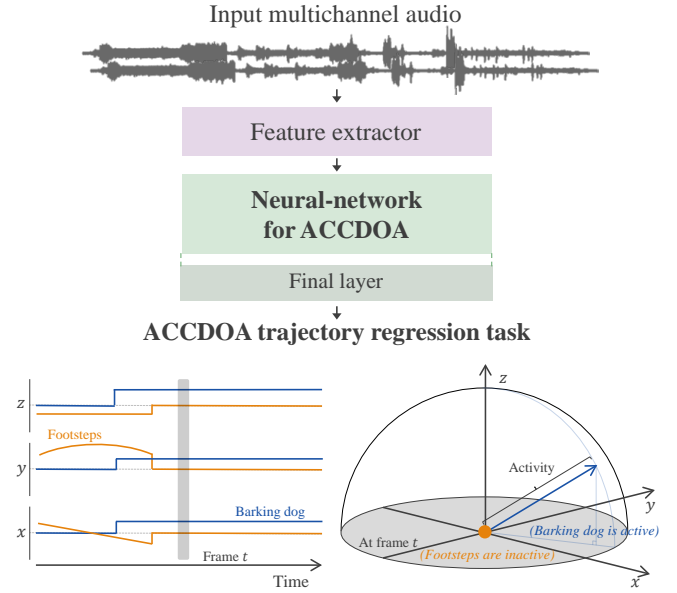


Fig. 1. To solve a SELD task with a single target, after the feature extraction, the network outputs frame-wise ACCDOA vectors for target sound events. The ACCDOA vector for each event assigns the activity to the length of the corresponding Cartesian DOA vector. When footsteps are inactive, and a barking dog is active at frame t , we get two ACCDOA vectors, as shown in the figure's lower right.

it also increases the system complexity and the network size. Keeping the network size small is important for edge devices.

To address the multi-objective problem while keeping the network size small, in this paper, we propose an activity-coupled Cartesian DOA (ACCDOA) representation for SELD. The ACCDOA representation assigns a sound event activity to the length of the corresponding Cartesian DOA vector, which enables us to handle a SELD task as a single task with a single network. The ACCDOA representation has two advantages: avoiding the multi-objective problem and network size increase. A schematic flow of the ACCDOA-based SELD system is shown in Fig. 1. After the feature extraction, the network outputs frame-wise ACCDOA vectors for target sound events. The model is trained to minimize the distance between the estimated and the target coordinates in the ACCDOA representation. When the target indicates no event, then the loss function is calculated only for the activity, not the DOA. In evaluations using the DCASE 2020 Task 3 dataset [14], the ACCDOA representation outperformed the two-branch representation in SELD metrics with fewer parameters. The ACCDOA-based SELD system also performed better than state-of-the-art SELD systems in terms of localization error and location-dependent F-score.

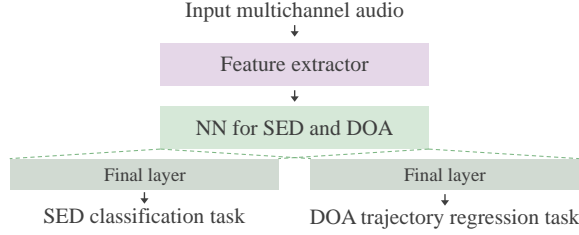


Fig. 2. SELDnet uses an SED target and a DOA target with a single network, which is trained to minimize a combined loss function.

2. RELATED WORK

We show an overview of the NN-based SELD methods [9–21], which can be categorized into two types of approaches. After that, we describe two methods closely related to the proposed method: SELDnet [13, 14] and the two-stage method [18].

2.1. Overview of NN-based SELD methods

First, we introduce approaches that integrate an NN-based SED method and a physics-based DOA estimation method [9–12]. Nguyen *et al.* used a convolutional recurrent neural-network (CRNN) for SED and a single-source histogram algorithm for DOA estimation and then integrated their results with a sequence matching network [9, 10]. Yasuda *et al.* refined an intensity-vector-based DOA estimation method by using NN-based denoising and source separation [11].

Second, we introduce approaches using only NN-based methods [13–21]. Recently, NN-based DOA estimation methods have performed outstandingly when labeled data have been available [23]. Also, this approach offers high performance in the SELD research area when we can use labeled data [7, 8].

Many NN-based methods have tackled a SELD task using a single network with multi objectives [13–17]. Adavanne *et al.* proposed SELDnet, which uses two targets: an SED target and a DOA target [13, 14]. The system of Wang *et al.* performed the best in the DCASE 2020 Task 3 competition, and they also used a SELDnet-like network architecture that uses an SED target and a DOA target [15].

A number of NN-based methods decomposed a SELD task into several subtasks and used subtask-specific networks [18–21]. Cao *et al.* proposed a two-stage method that uses two networks, i.e., an SED network and a DOA estimation network [18]. The system of Kapka and Lewandowski performed the best in the DCASE 2019 Task 3, and they also decomposed the SELD task into four tasks: estimating the number of active sources, estimating the DOA of a sound event when there is one active sound source, estimating the DOA when there are two, and classifying sound events with multi-labels [19].

2.2. SELDnet

We show the details of SELDnet [13], which is the first method that addresses the problem of localizing and recognizing more than two overlapping sound events simultaneously and tracking their activity per time frame. After the feature extraction, they use a CRNN architecture as an embedding network. As shown in Fig. 2, this is followed by two branches of fully-connected layers in parallel. One branch is for SED, and the other is for DOA estimation for each event class. Some papers show that using a Cartesian DOA format

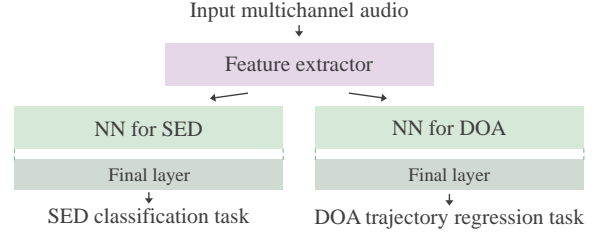


Fig. 3. The two-stage method uses two networks: an SED network and a DOA estimation network.

is better than using a spherical DOA format, i.e., azimuth and elevation, owing to the continuity [13, 23]. A binary-cross-entropy (BCE) loss is used between the SED predictions of SELDnet and reference sound class activities, while a mean squared error (MSE) loss is used for the DOA estimates of the SELDnet and the reference DOA. They combine the losses linearly with weights and search several weights to balance the losses during optimization.

2.3. Two-stage method

Fig. 3 shows the schematic diagram of the two-stage method [18], which uses two networks: an SED network and a DOA estimation network. After training only the SED network, a part of the network parameters is transferred from the SED network to the DOA estimation network. Then the DOA estimation network is trained. A BCE loss is also used between the SED network predictions and the reference. They adopted a masked MSE loss between the DOA estimates and the reference DOA. When an event is inactive, the MSE loss function is not calculated since it is not used in inference time. SELDnet for the DCASE 2020 Task 3 baseline [14] incorporates the masked MSE loss for its DOA branch.

3. PROPOSED METHOD

We formulate the ACCDOA representation with activity and Cartesian DOA and show how to use the ACCDOA representation for SELD.

3.1. ACCDOA representation

Let $\mathbf{a} \in \mathbb{R}^{C \times T}$ be C -class T -frame activities, whose reference value of each activity is 1 when an event is active and 0 when inactive, i.e., a reference activity $a_{ct}^* \in \{0, 1\}$. Also let $\mathbf{R} \in \mathbb{R}^{3 \times C \times T}$ be Cartesian DOAs, where the length of each Cartesian DOA is 1, i.e., $\|\mathbf{R}_{ct}\| = 1$ when a class c is active. $\|\cdot\|$ is Euclidean distance. Each C sound event class is represented by three nodes corresponding to the sound event location in x , y , and z axes.

Then we formulate the ACCDOA representation $\mathbf{P} \in \mathbb{R}^{3 \times C \times T}$ with activity and Cartesian DOA:

$$\mathbf{P}_{ct} = a_{ct} \mathbf{R}_{ct}. \quad (1)$$

Fig. 4 shows an example of the relationship between these representations. Also, activity and Cartesian DOA are obtained from the ACCDOA representation as follows:

$$a_{ct} = \|\mathbf{P}_{ct}\|, \quad (2)$$

$$\mathbf{R}_{ct} = \frac{\mathbf{P}_{ct}}{\|\mathbf{P}_{ct}\|} \quad (c \text{ is active}), \quad (3)$$

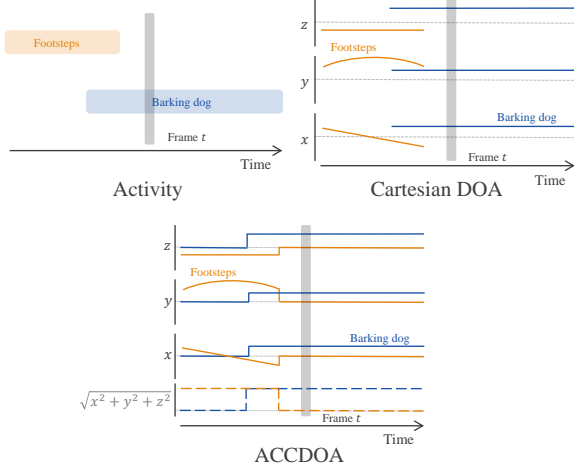


Fig. 4. The activity of each event class is represented by the length of the corresponding ACCDOA vector. When an event class is active, the DOA is also represented by the direction of the corresponding ACCDOA vector.

where a Cartesian DOA is considered only when the event class is active. When estimating, we use threshold processing to determine whether an event class is active or not.

3.2. SELD with ACCDOA representation

We use a CRNN architecture as an embedding network, $\mathcal{F}_{\text{embed}, \theta'(\cdot)}$, where θ' is the network parameters. Let $\mathbf{X} \in \mathbb{R}^{M \times F \times T'}$ be an input consisting of M -channel F -dimensional T' -frame acoustic features.

$$\mathbf{E} = \mathcal{F}_{\text{embed}, \theta'}(\mathbf{X}), \quad (4)$$

where $\mathbf{E} \in \mathbb{R}^{K \times T}$ is an embedding vector for the input, K is the number of dimensions of the embedding space.

Using ACCDOA, we can define a SELD task as an ACCDOA estimation problem. The embedding vector is followed by only one fully-connected layer to estimate ACCDOA representation vectors, $\mathcal{F}_{\text{ACCCDOA}, \theta}(\cdot)$, where θ is the parameters.

$$\hat{\mathbf{P}}_t = \mathcal{F}_{\text{ACCCDOA}, \theta}(\mathbf{E}_t), \quad (5)$$

where $\hat{\mathbf{P}}$ is an estimated ACCDOA representation. We estimate SELD outputs without two task-specific branches or two task-specific networks. That leads to simple network architecture and small network size.

Fig. 5 shows an example of the differences between reference and estimated ACCDOA at frame t in Fig. 4. We use MSE as a single loss function for a SELD task.

$$l_{\text{ACCCDOA}} = \frac{1}{CT} \sum_c \sum_t \text{MSE}(\mathbf{P}_{ct}^*, \hat{\mathbf{P}}_{ct}), \quad (6)$$

where \mathbf{P}^* is a reference ACCDOA representation. When the ground truth indicates no event, then the MSE loss function is calculated only for the activity, not the DOA. In the original SELDnet [13], even in the case of no event, DOA loss needed to be calculated. Using ACCDOA can avoid such calculations, as can using masked MSE. Activity is no longer interpreted as a posterior probability because BCE is not used. However, threshold processing can be performed in the same manner. This single loss enables us to avoid the multi-objective problem and focus on other hyper-parameter tunings.

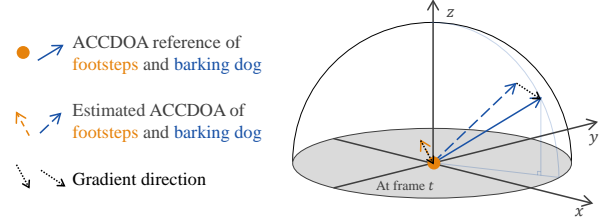


Fig. 5. ACCDOA vectors at frame t in Fig. 4. A Solid line or a dot shows an ACCDOA reference, whose length is 1 when an event is active and 0 when inactive. Dashed lines show ACCDOA estimated by a network, which is trained to bring the estimation closer to the reference. Dotted lines depict the gradient directions.

4. EXPERIMENTAL EVALUATION

We evaluated the ACCDOA representation and the two-branch representation using TAU Spatial Sound Events 2020 with the setup for DCASE 2020 Task 3 [14]. We also compared our proposed method with state-of-the-art SELD systems without model ensembles.

4.1. Task setups

We used the development set of TAU Spatial Sound Events 2020 - Ambisonic with the suggested setup for DCASE 2020 Task 3 [14]. The dataset contained 600 one-minute sound scene recordings: 400 for training, 100 for validation, and 100 for testing. The sound scene recordings were synthesized by adding sound event samples convolved with room impulse response (RIR) to spatial ambient noise. The sound event samples were from the NIGENS general sound events database [24], which consisted of 14 event classes such as footsteps and a barking dog. The RIRs and ambient noise recordings were collected at 15 different indoor locations. Each event had an equal probability of being either static or moving. The moving sound events were synthesized with 10, 20, or 40 degrees per second. Signal-to-noise ratios ranged from 6 dB to 30 dB.

Following the setup, four metrics were used for the evaluation [25]. The first was the localization error LE_{CD} , which expresses the average angular distance between the same class's predictions and references. The second was a simple localization recall metric LR_{CD} , which tells the true positive rate of how many of these localization estimates were detected in a class out of the total number of class instances. The next two metrics were the location-dependent error rate ER_{20° and F-score F_{20° , where predictions were considered true positives only when the distance from the reference was less than 20° .

4.2. Experimental settings

We compared the ACCDOA representation with the two-branch representations for SELDnet (Two-branch for SELDnet) and the two-stage method (Two-branch for Two-stage). The differences between ACCDOA and Two-branch for SELDnet were only after the embedding vector. Following the baseline for DCASE 2020 Task 3, each task-specific branch for SELDnet had two fully-connected layers, and the loss functions were BCE and masked MSE. The loss weight value was 10, chosen from 1, 5, 10, 20, 100. Also, the differences between ACCDOA and Two-branch for Two-stage were the number of networks. In both representations, other system configurations such as feature extraction, data augmentation, and post-processing mostly followed our DCASE 2020 challenge settings [26].

Table 1. SELD performance with two types of CRNNs in different representations evaluated for the DCASE 2020 Task 3 development set.

Network	Representation	Number of parameters	Validation split				Testing split			
			LE_{CD}	LR_{CD}	ER_{20°	F_{20°	LE_{CD}	LR_{CD}	ER_{20°	F_{20°
CRNN	Two-branch for SELDnet	5.24 M	9.6°	78.7	0.38	72.5	11.0°	70.9	0.45	64.1
	Two-branch for Two-stage	9.41 M	8.9°	79.5	0.36	74.3	10.9°	73.0	0.44	66.3
	ACCDOA (proposed)	4.71 M	8.5°	76.0	0.39	72.4	9.6°	71.9	0.43	67.5
RD3Net	Two-branch for SELDnet	1.62 M	9.2°	83.1	0.33	77.1	11.6°	79.7	0.38	70.7
	Two-branch for Two-stage	3.12 M	8.0°	83.0	0.32	78.5	9.7°	76.2	0.39	70.5
	ACCDOA (proposed)	1.56 M	7.6°	83.6	0.28	80.9	8.3°	77.5	0.36	74.2

Multichannel amplitude spectrograms and inter-channel phase differences (IPDs) were used as frame-wise features. Since the input consists of four-channel signals, we extracted four amplitude spectrograms and three IPDs.

Following Takahashi *et al.* [27, 28], we applied the equalized mixture data augmentation (EMDA) method where up to two sound events are mixed with random amplitudes, delays, and modulations of frequency characteristics, i.e., equalization. We also adopted the spatial augmentation method of Mazzon *et al.* [29], which rotates the training data represented in the first-order Ambisonic (FOA) format. We used the multichannel version of SpecAugment [26]. In addition to the time-frequency hard-masking schemes [30] applied to amplitude spectrograms, the masking schemes were extended to the channel dimension [26]. The target channel for the channel masking, m_0 , was chosen from $[0, M)$ where M denotes the number of microphone channels. For the IPD features, instead of multiplying a mask value by the original value, the actual values were replaced with random values, where the values were sampled from a uniform distribution ranging from 0 to 2π .

We prepared two types of CRNNs: a conventional CRNN used in [18] and RD3Net [31]. RD3Net has shown state-of-the-art performance in music source separation, and the advantage is the efficiency of modeling a large receptive field, which is beneficial for many tasks that require a long context for an accurate prediction [31]. The adaptation to the SELD task includes three modifications. First, we omitted dense blocks in the up-sampling path because high frame-rate prediction is unnecessary for the SELD task. Second, we placed gated recurrent unit (GRU) cells existing only in the bottleneck part. Third, the batch normalization was replaced with the network deconvolution [32]. In each dense block, the initial convolution’s dilation factor was set to one, and the dilation factor doubled every time the next convolution was applied.

We split the 60-second input audio into shorter segments with overlap during the inference, processed each segment, and averaged the results of overlapped frames. To further improve the performance, we conducted post-processing with the following procedure: rotating the FOA data, estimating the ACCDOA vectors, rotating the vectors back, and averaging the vectors of different rotation patterns.

The sampling frequency was set to 24 kHz. The short-term Fourier transform (STFT) was applied with a configuration of 20 ms frame length and 10 ms frame hop. The frame length of the network input was 128 frames. During the inference time, the frame shift length was set to 20 frames. We used a batch size of 32, and each training sample was generated on-the-fly [33]. The learning rate was set to 0.001 and decayed 0.9 times every 20,000 iterations. We used the Adam optimizer with a weight decay of 10^{-6} .

We also compared our proposed method with state-of-the-art SELD systems without model ensembles. In this case, to further improve the performance, we used RD3Net and extended the network input’s frame length to 1,024 frames.

Table 2. SELD performance of state-of-the-art systems and our ACCDOA-based system for the development set. PP denotes post-processing described in Sec. 4.2.

System	# of params	Testing split			
		LE_{CD}	LR_{CD}	ER_{20°	F_{20°
Wang’s [15]	N/A	9.4°	82.8	0.29	76.4
Nguyen’s [10]	2.28 M	13.5°	81.5	0.38	69.4
FOA Baseline [14]	0.51 M	22.8°	60.7	0.72	37.4
Ours w/o PP	1.56 M	10.2°	79.1	0.36	73.0
Ours	1.56 M	7.9°	80.5	0.32	76.8

4.3. Experimental results

Table 1 shows the performance with two types of CRNNs in different representations. As shown in the table, the ACCDOA representation has fewer parameters than two-branch representations. The ACCDOA representation outperformed the two-branch representation for SELDnet for most metrics with both networks. While the ACCDOA representation showed 1.0 point higher LR_{CD} than the Two-branch for SELDnet in the testing split with CRNN, the ACCDOA representation improved F_{20° by 3.4 points. This result suggests that the ACCDOA representation is more effective in improving location-dependent detection. Our experimental results show that the ACCDOA representation can simultaneously focus on estimating activity and DOA with a single target using a single network.

Table 2 shows the performances of the SELD systems without model ensembles. Our ACCDOA-based system performed the best in terms of LE_{CD} and F_{20° for the DCASE 2020 Task 3 development set with small number of parameters. The results also show the post-processing especially improves localization performance.

The dataset used in the experiments can contain up to two overlapping sound event classes, and almost all overlaps are those of different classes. In the future, when we need to tackle overlaps of the same class, a promising way is to incorporate a multi-track extension [9, 10, 21] to the ACCDOA representation.

5. CONCLUSION

We proposed the activity-coupled Cartesian direction-of-arrival (ACCDOA) representation, which assigns a sound event activity to the length of a corresponding Cartesian DOA vector for sound event localization and detection (SELD). The ACCDOA representation enables us to solve a SELD task with a single target using a single network. The ACCDOA representation avoids the necessity of balancing objectives for sound event detection (SED) and DOA estimation and the increase of network size. In the evaluations on the SELD task for DCASE 2020 Task 3, the ACCDOA representation outperformed the conventional two-branch representations in the joint SELD metrics with fewer parameters. The ACCDOA-based system also performed better than state-of-the-art systems in terms of localization error and location-dependent F-score.

6. REFERENCES

- [1] M. Crocco, M. Cristani, A. Trucco, and V. Murino, "Audio surveillance: A systematic review," *ACM Computing Surveys*, vol. 48, no. 4, pp. 1–46, 2016.
- [2] C. Grobler, C. P. Kruger, B. J. Silva, and G. P. Hancke, "Sound based localization and identification in industrial environments," in *Proc. of IEEE IECON*, 2017, pp. 6119–6124.
- [3] G. Valenzise, L. Gerosa, M. Tagliasacchi, F. Antonacci, and A. Sarti, "Scream and gunshot detection and localization for audio-surveillance systems," in *Proc. of IEEE AVSS*, 2007, pp. 21–26.
- [4] S. Chu, S. Narayanan, and C.-C. J. Kuo, "Environmental sound recognition with time–frequency audio features," *IEEE Trans. on ASLP*, vol. 17, no. 6, pp. 1142–1158, 2009.
- [5] R. Takeda and K. Komatani, "Sound source localization based on deep neural networks with directional activate function exploiting phase information," in *Proc. of IEEE ICASSP*, 2016, pp. 405–409.
- [6] N. Yalta, K. Nakadai, and T. Ogata, "Sound source localization using deep learning models," *Journal of Robotics and Mechatronics*, vol. 29, no. 1, pp. 37–48, 2017.
- [7] S. Adavanne, A. Politis, and T. Virtanen, "A multi-room reverberant dataset for sound event localization and detection," in *Proc. of DCASE workshop*, 2019.
- [8] A. Politis, A. Mesaros, S. Adavanne, T. Heittola, and T. Virtanen, "Overview and evaluation of sound event localization and detection in DCASE 2019," *arXiv:2009.02792*, 2020.
- [9] T. N. T. Nguyen, D. L. Jones, and W.-S. Gan, "A sequence matching network for polyphonic sound event localization and detection," in *Proc. of IEEE ICASSP*, 2020, pp. 71–75.
- [10] —, "DCASE 2020 Task 3: Ensemble of sequence matching networks for dynamic sound event localization, detection, and tracking," in *Tech. report of DCASE Challenge*, 2020.
- [11] M. Yasuda, Y. Koizumi, S. Saito, H. Uematsu, and K. Imoto, "Sound event localization based on sound intensity vector refined by DNN-based denoising and source separation," in *Proc. of IEEE ICASSP*, 2020, pp. 651–655.
- [12] W. Xue, T. Ying, Z. Chao, and D. Guohong, "Multi-beam and multi-task learning for joint sound event detection and localization," in *Tech. report of DCASE Challenge*, 2019.
- [13] S. Adavanne, A. Politis, J. Nikunen, and T. Virtanen, "Sound event localization and detection of overlapping sources using convolutional recurrent neural networks," *IEEE JSTSP*, vol. 13, no. 1, pp. 34–48, 2018.
- [14] A. Politis, S. Adavanne, and T. Virtanen, "A dataset of reverberant spatial sound scenes with moving sources for sound event localization and detection," *arXiv:2006.01919*, 2020.
- [15] Q. Wang, H. Wu, Z. Jing, F. Ma, Y. Fang, Y. Wang, T. Chen, J. Pan, J. Du, and C.-H. Lee, "The USTC-iFLYTEK system for sound event localization and detection of DCASE2020 challenge," in *Tech. report of DCASE Challenge*, 2020.
- [16] D. Communiello, M. Lella, S. Scardapane, and A. Uncini, "Quaternion convolutional neural networks for detection and localization of 3D sound events," in *Proc. of IEEE ICASSP*, 2019, pp. 8533–8537.
- [17] H. Phan, L. Pham, P. Koch, N. Q. Duong, I. McLoughlin, and A. Mertins, "On multitask loss function for audio event detection and localization," *arXiv:2009.05527*, 2020.
- [18] Y. Cao, Q. Kong, T. Iqbal, F. An, W. Wang, and M. D. Plumbley, "Polyphonic sound event detection and localization using a two-stage strategy," in *Proc. of DCASE Workshop*, 2019.
- [19] S. Kapka and M. Lewandowski, "Sound source detection, localization and classification using consecutive ensemble of crnn models," in *Proc. of DCASE Workshop*, 2019.
- [20] J. Zhang, W. Ding, and L. He, "Data augmentation and prior knowledge-based regularization for sound event localization and detection," in *Tech. Report of DCASE Challenge*, 2019.
- [21] Y. Cao, T. Iqbal, Q. Kong, Y. Zhong, W. Wang, and M. D. Plumbley, "Event-independent network for polyphonic sound event localization and detection," *arXiv:2010.00140*, 2020.
- [22] A. Dosovitskiy and J. Djolonga, "You Only Train Once: Loss-conditional training of deep networks," in *Proc. of ICLR*, 2020.
- [23] Z. Tang, J. D. Kanu, K. Hogan, and D. Manocha, "Regression and classification for direction-of-arrival estimation with convolutional recurrent neural networks," in *Proc. of Interspeech*, 2019, pp. 654–658.
- [24] I. Trowitzsch, J. Taghia, Y. Kashef, and K. Obermayer, "The NIGENS general sound events database," *arXiv:1902.08314*, 2019.
- [25] A. Mesaros, S. Adavanne, A. Politis, T. Heittola, and T. Virtanen, "Joint measurement of localization and detection of sound events," in *Proc. of IEEE WASPAA*, 2019.
- [26] K. Shimada, N. Takahashi, S. Takahashi, and Y. Mitsufuji, "Sound event localization and detection using activity-coupled Cartesian DOA vector and RD3Net," in *Tech. report of DCASE Challenge*, 2020.
- [27] N. Takahashi, M. Gygli, B. Pfister, and L. V. Gool, "Deep convolutional neural networks and data augmentation for acoustic event detection," in *Proc. of Interspeech*, 2016, pp. 2982–2986.
- [28] N. Takahashi, M. Gygli, and L. Van Gool, "AENet: Learning deep audio features for video analysis," *IEEE Trans. on Multimedia*, vol. 20, pp. 513–524, 2017.
- [29] L. Mazzon, Y. Koizumi, M. Yasuda, and N. Harada, "First order ambisonics domain spatial augmentation for DNN-based direction of arrival estimation," in *Proc. of DCASE Workshop*, 2019.
- [30] D. S. Park, W. Chan, Y. Zhang, C.-C. Chiu, B. Zoph, E. D. Cubuk, and Q. V. Le, "SpecAugment: A simple data augmentation method for automatic speech recognition," in *Proc. of Interspeech*, 2019, pp. 2613–2617.
- [31] N. Takahashi and Y. Mitsufuji, "D3Net: Densely connected multidilated densenet for music source separation," *arXiv:2010.01733*, 2020.
- [32] C. Ye, M. Evanusa, H. He, A. Mitrokhin, T. Goldstein, J. A. Yorke, C. Fermuller, and Y. Aloimonos, "Network deconvolution," in *Proc. of ICLR*, 2020.
- [33] H. Erdogan and T. Yoshioka, "Investigations on data augmentation and loss functions for deep learning based speech-background separation," in *Proc. of Interspeech*, 2018, pp. 3499–3503.